

17. Mochida, M., Kitamori, Y., Kawamura, K., Nojiri, Y. & Suzuki, K. Fatty acids in the marine atmosphere: Factors governing their concentrations and evaluation of organic films on sea salt particles. *J. Geophys. Res.* **107**, doi:10.1029/2001JD001278 (2002).
18. Oppo, C. *et al.* Surfactant component of marine organic matter as agents for biogeochemical fractionation of pollutants transport via marine aerosol. *Mar. Chem.* **63**, 235–253 (1999).
19. Landrath, D. C. Bubble scavenging and the water to air transfer of organic material in the sea. *Adv. Chem. Ser.* **145**, 360–387 (1976).
20. Geever, M. *et al.* Measurements of primary marine aerosol fluxes at Mace Head, Ireland. In Abstracts of European Aerosol Conference, Madrid, 2003, Vol. 1 *J. Aer. Sci.* S637–S638 (2003).
21. Martensson, E. M., Nilsson, E. D., de Leeuw, G., Cohen, L. H. & Hansson, H. C. Laboratory simulations and parameterization of the primary marine aerosol production. *J. Geophys. Res.* **108**, doi:10.1029/2002JD002263 (2003).
22. Facchini, M. C., Mircea, M., Fuzzi, S. & Charlson, R. J. Cloud albedo enhancement by surface-active organic solutes in growing droplets. *Nature* **401**, 257–259 (1999).
23. Nenes, A. *et al.* Can chemical effects on cloud droplet number rival the first indirect effect? *Geophys. Res. Lett.* **29**, doi: 10.1029/2002GL015295 (2002).
24. Beardall, J. & Raven, J. A. The potential effects of global climate change on microalgal photosynthesis, growth and ecology. *Phycologia* **43**, 26–40 (2004).

**Supplementary Information** accompanies the paper on [www.nature.com/nature](http://www.nature.com/nature).

**Acknowledgements** This work was partly supported by the European Commission (Projects QUEST and PHOENICS), Irish Research Council for Science, Engineering and Technology, and the Irish Higher Education Authority, Italian Ministry of Environment (Italy–USA Cooperation on Science and Technology of Climate Change). SeaWiFS chlorophyll products were provided by the SeaWiFS project, NASA/Goddard Space Flight Center and ORBIMAGE.

**Competing interests statement** The authors declare that they have no competing financial interests.

**Correspondence** and requests for materials should be addressed to M.C.F. (mc.facchini@isac.cnr.it).

## Basal tyrannosauroids from China and evidence for protofeathers in tyrannosauroids

Xing Xu<sup>1\*</sup>, Mark A. Norell<sup>2</sup>, Xuewen Kuang<sup>3</sup>, Xiaolin Wang<sup>1</sup>, Qi Zhao<sup>1</sup> & Chengkai Jia<sup>1</sup>

<sup>1</sup>Institute of Vertebrate Paleontology and Paleoanthropology, Chinese Academy of Sciences, Beijing 100044, China

<sup>2</sup>American Museum of Natural History, New York 10024, USA

<sup>3</sup>Tianjin Museum of Natural History, Tianjin 300074, China

\* Present address: American Museum of Natural History, Central Park West at 79th Street, New York City, New York 10024, USA

Tyrannosauroids are one of the last and the most successful large-bodied predatory dinosaur groups<sup>1–5</sup>, but their early history remains poorly understood. Here we report a new basal tyrannosauroid from the Early Cretaceous Yixian Formation of western Liaoning, China, which is small and gracile and has relatively long arms with three-fingered hands. The new taxon is the earliest known unquestionable tyrannosauroid found so far<sup>6–9</sup>. It shows a mosaic of characters, including a derived cranial structure resembling that of derived tyrannosauroids<sup>1–5</sup> and a primitive postcranial skeleton similar to basal coelurosaurians. One of the specimens also preserves a filamentous integumentary covering similar to that of other coelurosaurian theropods from western Liaoning. This provides the first direct fossil evidence that tyrannosauroids had protofeathers.

Theropoda Marsh, 1881  
Coelurosauria *sensu* Gauthier, 1986  
Tyrannosauroida Osborn, 1905  
*Dilong paradoxus* gen. et sp. nov.

**Etymology.** The generic name is derived from Chinese *di*

(emperor) + *long* (dragon). The specific name refers to the surprising characters of this animal.

**Holotype.** A semi-articulated skeleton including an almost complete skull, IVPP (Institute of Vertebrate Paleontology and Paleoanthropology, Beijing) V14243.

**Referred material.** IVPP V14242, a nearly complete skull and associated presacral vertebrae; TNP01109 (in collections of Tianjin Museum of Natural History), a partial skull. IVPP V11579 is here referred to this taxon; however, on further analysis it may be determined that it represents a second, closely related species of *Dilong*.

**Horizon and locality.** Lujiatun, Beipiao, western Liaoning; older than 128 and younger than 139 million years fine sand beds of the lower part of the Yixian Formation<sup>10</sup>.

**Diagnosis.** A small tyrannosauroid distinguishable from other tyrannosauroids by the unique presence of two large pneumatic recesses dorsal to the antorbital fossa on the maxilla, a Y-shaped crest formed by the nasals and lacrimals, an extremely long descending process of the squamosal extending close to the mandibular articulation of the quadrate, a lateral projection of the basisphenoid anterior to the basal tuber, very deep, sub-circular interspinous ligamentous fossae on cervical vertebrae, robust scapula with a wide distal end (distal end twice as wide as the proximal scapular blade) and a hypertrophied coracoid (dorsoventral length about 70% of the scapular length).

*Dilong paradoxus* is a small tyrannosauroid (see Supplementary Information for ontogenetic assessments and measurements of the specimens). IVPP V14243, the largest of the known specimens, is estimated to be 1.6 m in body length. The small size of *Dilong paradoxus*, in comparison with more derived, large tyrannosauroids, is consistent with the trend of size increase reported for this clade<sup>7,9,11</sup>. *Dilong paradoxus* shares numerous derived cranial similarities with other tyrannosauroids (Fig. 1a–f)<sup>1–5,12</sup>. The premaxilla has a deep subnasal body. The anterior ventral edge of the maxilla is convex, and dorsally the maxilla clearly excludes the nasal from participating in the antorbital fossa, a unique feature to tyrannosauroids<sup>13</sup>. In lateral view, a small promaxillary fenestra is visible anteroventral to the maxillary fenestra at the anterior margin of the antorbital fossa. The nasals are fused at an early ontogenetic stage, as in a few theropods and other tyrannosauroids<sup>1–5,14</sup>, but they are more similar to other tyrannosauroids because of their convex dorsal surface<sup>1,3</sup>. The pneumatic lacrimal is robust. The descending process of the lacrimal is evidently concave along the orbital edge in lateral view; anteroventrally it floors the antorbital fossa with the maxilla and jugal. The jugal is anteriorly pneumatic and contributes significantly to the border of the antorbital fenestra. Right under the orbit, the ventral margin of the jugal is bent and thickened, forming a well-developed corneal process. The prefrontal is reduced, although it still separates the posterior margin of the lacrimal from the frontal. The supratemporal fossae, separated by a low sagittal crest, extend extensively onto the frontals, occupying large portions of their lateroposterior edges. The lateral nuchal crest is fairly high relative to most other theropods. The quadratojugal is massive and dorsally expanded modestly, suggesting the presence of a weak quadratojugal–squamosal flange dividing the lateral temporal fenestra. The quadrate is posterodorsally orientated and has a pneumatic opening on the posterior surface as in many coelurosaurians<sup>15</sup>. The supraoccipital ridge is prominent and the paroccipital process is laterally directed. The basicranium is extensively pneumatized, with a deep basisphenoidal recess that contains large foramina, and is posterovertrally orientated. The mandibular fenestra, if present, must be extremely small. The articular is pneumatic and has a reduced retroarticular process that is orientated posteriorly. A long supracondylar process is present; however, because of preservation it is not apparent if it was fused to a separate coronoid. As in other tyrannosauroids<sup>1,3</sup>, the premaxillary teeth are closely packed and more mediolaterally than anteroposteriorly orientated. They are

D-shaped, serrated, and much smaller than the maxillary teeth. The maxillary and dentary teeth (Fig. 1f) are strongly laterally compressed and, as in velociraptorines<sup>16</sup>, *Eotyrannus*<sup>8</sup> and juvenile tyrannosaurids<sup>13</sup>, have posterior serrations that are significantly larger than the anterior ones. Different from most tyrannosauroids, *Dilong paradoxus* has a less robust skull, a much larger external naris, an expanded braincase, a lower sagittal crest, an antero-posteriorly longer basicranium and a smaller mylohyoid foramen, and lacks a surangular foramen (Fig. 1a–e). Some of these features might be size related; however, progressively larger size is a phylogenetic trend in tyrannosaurids<sup>7,9,11</sup>. It is also different from other tyrannosauroids in several unique features. In lateral view, the maxilla is depressed dorsal to the well-defined dorsal edge of the antorbital fossa. Within this longitudinal depression are two large pneumatic recesses. In dorsal view, a Y-shaped crest is present, which is formed by the nasals and lacrimals. The descending process

of the squamosal is extremely long and ventrally extends approximately to the level of the mandibular articulation of the quadrate. Anterior to the basal tuber, the basisphenoid projects laterally to form a lateral projection, a feature unknown in other tyrannosauroids. These features contribute to the cranial diagnosis for the new taxon.

Postcranially *Dilong paradoxus* has proportionally a longer neck and trunk. The opisthocoelous cervical vertebrae have low neural spines and large pneumatic openings on relatively shallow centra (Fig. 1g, h), the posterior dorsal vertebrae have much larger, relatively long and non-pneumatic amphicoelous centra, transversely narrow neural spines, and strap-like broad transverse processes, and the distal caudal vertebrae lack transverse processes and neural spines. Very deep, subcircular interspinous ligamentous fossae are present on cervical vertebrae. In some theropods such as *Allosaurus*<sup>16</sup>, the ligament fossae are well developed but are much shallower and

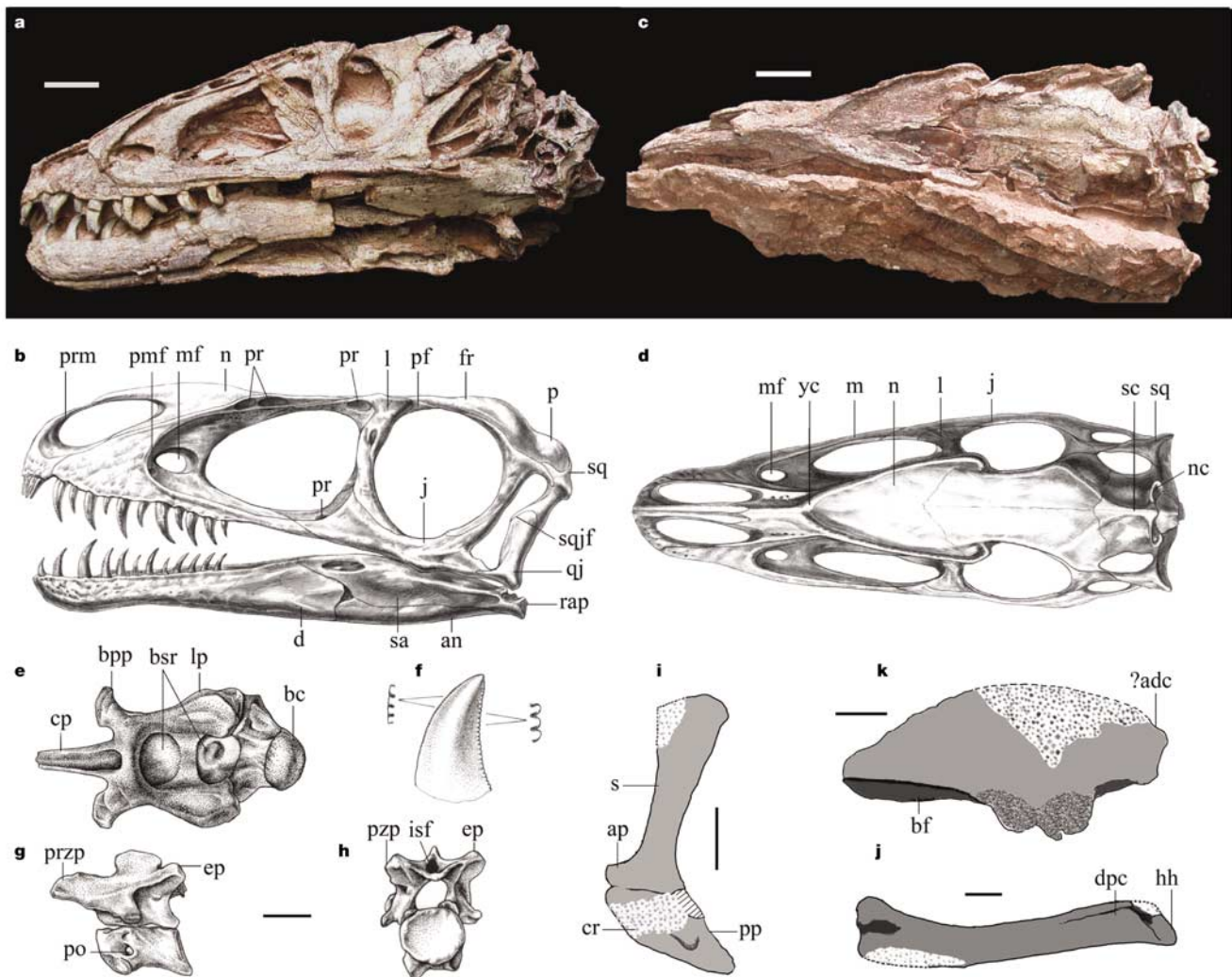


**Figure 1** *Dilong paradoxus*. **a, c**, Photographs of the skull of IVPP V14243 in left lateral (**a**) and dorsal (**c**) views. Scale bar, 2 cm. **b, d**, Cranial reconstruction in left lateral (**b**) and dorsal (**d**) views. **e**, Braincase of IVPP V14242 in ventral view. **f**, A dentary tooth of IVPP V14242 in lingual view, with detailed views of the anterior and posterior margins. **g, h**, A middle cervical vertebra of IVPP V14242 in left lateral (**g**) and posterior (**h**) views. Scale bar, 1 cm. **i**, Left scapula and coracoid of IVPP V14243 in lateral view. Scale bar, 2 cm. **j**, Left humerus of IVPP V14243 in anterior view. Scale bar, 1 cm. **k**, Left ilium of IVPP V14243 in medial view. The acetabular region is crushed. Scale bar, 2 cm. Abbreviations: ?adc, ?anterodorsal concavity; an, angular; ap, acromion process; bc, basioccipital

condyle; bf, brevis fossa; bpp, basiopterygoid process; bsr, basisphenoid recess; cp, cultriform process; cr, coracoid; d, dentary; dpc, deltopectoral crest; ep, epiphysis; fr, frontal; hh, humeral head; isf, interspinous ligamentous fossa; j, jugal; l, lacrimal; lp, lateral process; m, maxilla; mf, maxillary fenestra; n, nasal; nc, nuchal crest; p, parietal; pf, prefrontal; pmf, promaxillary fenestra; po, pneumatic opening; pp, posterior process; pr, pneumatic recess; prm, premaxilla; przp, prezygapophysis; pzp, postzygapophysis; qj, quadratojugal; rap, retroarticular process; s, scapula; sa, surangular; sc, sagittal crest; sq, squamosal; sqjf, squamosal–quadratojugal flange; yc, Y-shaped crest.

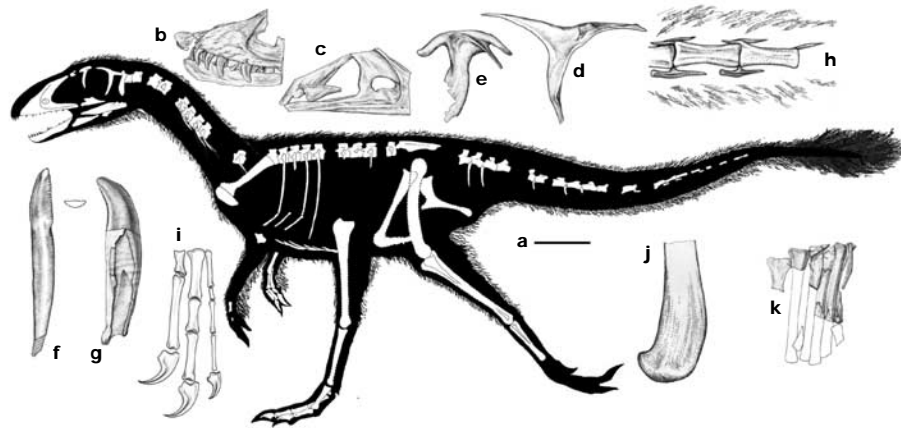


**Figure 2** IVPP V11579. **a**, Skeletal reconstruction showing preserved bones. **b**, Left maxilla in lateral view. **c**, Right maxilla in lateral view. **d**, Left postorbital in medial view. **e**, Right squamosal in lateral view. **f**, Premaxillary tooth in lingual view. Note the flat lingual

surface. **g**, Maxillary tooth in labial view. **h**, Distal caudal vertebrae associated with branched integumentary structures. **i**, Reconstructed left manus in dorsal view. **j**, Left ischium in lateral view. **k**, Left metatarsals in anterior view. Scale bar, 10 cm (**a**).

more groove-like. The scapula is robust, with a distal end about twice as wide as the proximal scapular blade. The acromion process of the scapula is dorsally extended significantly. The coracoid is hypertrophied and is about 70% of the scapular length (Fig. 1i). The humerus is more than half of the femoral length and is significantly longer than the scapula, a feature seen in some derived maniraptorans<sup>15</sup>. As in other tyrannosauroids<sup>5</sup>, the proximal half of the humerus is narrow, with a proximal end that is only slightly differentiated (Fig. 1j). The distal end of the radius is flattened. The pelvis is less robust than in other tyrannosauroids. The ilium is considerably shorter than the femur and is similar to that of maniraptorans in having a tapering posterior blade and it lacks a broad ventral hook-like projection from the anterior blade (Fig. 1k)<sup>1,18</sup>. The pubis has an extremely large pubic boot (more than half the pubic length)<sup>1</sup>, but with little anterior extension. The hindlimb proportions indicate cursorial capability, with tibia/femur and metatarsus/femur ratios of 1.13 and 0.66, respectively. However, considering the allometric growth in the tyrannosauroid development<sup>19,20</sup>, it has shorter lower legs than in similar-sized tyrannosauroids. The wing-like lesser trochanter of the femur is significantly lower than the femoral head. As in derived dromaeosaurids<sup>15</sup>, the metatarsus is relatively robust. Unlike other tyrannosauroids<sup>19</sup>, metatarsal III is proximally unconstricted and weakly distally ginglymoid. Metatarsal V is elongate, though not to the same degree as in dromaeosaurids<sup>15</sup>.

IVPP V14242 is smaller than IVPP V14243 and represents an earlier ontogenetic stage than the latter. It differs from IVPP V14243 in having smaller external nares, more posteriorly positioned maxillary fenestrae, a more expanded braincase, a more slender ventral process of the squamosal, a less developed and more posteriorly located lateral process of the basisphenoid and a longer retroarticular process, and in lacking a sagittal crest and a nuchal crest.

A fragmentary specimen (IVPP V11579), which was collected from approximately 125-million-year-old grey shale of the Yixian Formation<sup>10</sup> of Zhangjiagou locality, Beipiao, western Liaoning, can be referred to *Dilong* on the basis of the identical morphologies of most overlapping elements, including squamosals, dentaries, splenials, teeth, cervical vertebrae, dorsal vertebrae, caudal vertebrae, and metatarsals (Fig. 2). IVPP V11579 provides additional significant information unavailable in the known specimens of *Dilong paradoxus*. The preserved manual elements show a robust manual digit II where metacarpal II and associated phalanges are much more robust than metacarpal I and corresponding phalanges. This is a derived feature also seen in other tyrannosauroids<sup>5</sup>. Manual digit

III, however, is not reduced in phalangeal number or digit length, though extremely slender, representing a precursor to the reduced manual digit III in more advanced tyrannosauroids<sup>1</sup>. The relatively long arms with three-fingered hands in Liaoning tyrannosauroids conform to predictions of current phylogenetic hypotheses about the morphology of basal tyrannosauroids<sup>7,21</sup>. In contrast with the derived tyrannosauroids<sup>1</sup> but similar to many basal coelurosaurians<sup>21</sup>, the distal end of the ischium is slightly expanded and curved anteriorly.

On the tail, traces of filamentous integumentary structures are preserved at an angle of about 30–45° to the caudal vertebral series (Fig. 3). A small patch of filamentous integumentary structures is also preserved close to the posterior left mandible. Those attached to the distal caudal vertebrae are more than 20 mm in length. They are branched but the pattern is difficult to discern. They seem to be composed of a series of filaments joined at their bases along a central filament as in *Sinornithosaurus*<sup>22</sup>. Many of these structures seem to be distally branched, as can be observed in some cases in *Sinornithosaurus* (IVPP V12811).

The fossil record of the tyrannosauroids is mainly restricted to the Late Cretaceous of North America and central and eastern Asia<sup>1–5</sup>. Several Early Cretaceous and Late Jurassic taxa have been reported, but they are either represented by limited material or are questionably referable<sup>6–9</sup>. Liaoning tyrannosauroids represent the most basal tyrannosauroid species (see Supplementary Information for a numerical cladistic analysis) represented by multiple, nearly complete specimens found so far and provide new insights into the early evolution of tyrannosauroid dinosaurs.

Comparatively, Liaoning tyrannosauroids are similar to other juvenile tyrannosauroids; for example, they both have long and low proportions of snout and mandible, teeth with differently sized anterior and posterior serrations, low cervical neural spines, relatively low cervical and dorsal centra, and dorsal centra much larger than cervical ones<sup>13,23</sup>. Some of these features have also been reported in other basal tyrannosauroids<sup>8</sup>. These data indicate that peramorphosis might be important in tyrannosauroid evolution, pending an analysis on a more complete data set.

Liaoning tyrannosauroids show more of the derived modifications of tyrannosauroids in the cranium than postcranium. This might also be so in *Eotyrannus*<sup>8</sup>. For example, Liaoning tyrannosauroids have 80% cranial diagnostic features relative to 25% postcranial synapomorphies of tyrannosauroids (see Supplementary Information)<sup>1–4</sup>. This indicates that the cranial modification occurred earlier than the postcranial modification in tyrannosauroid evolution.

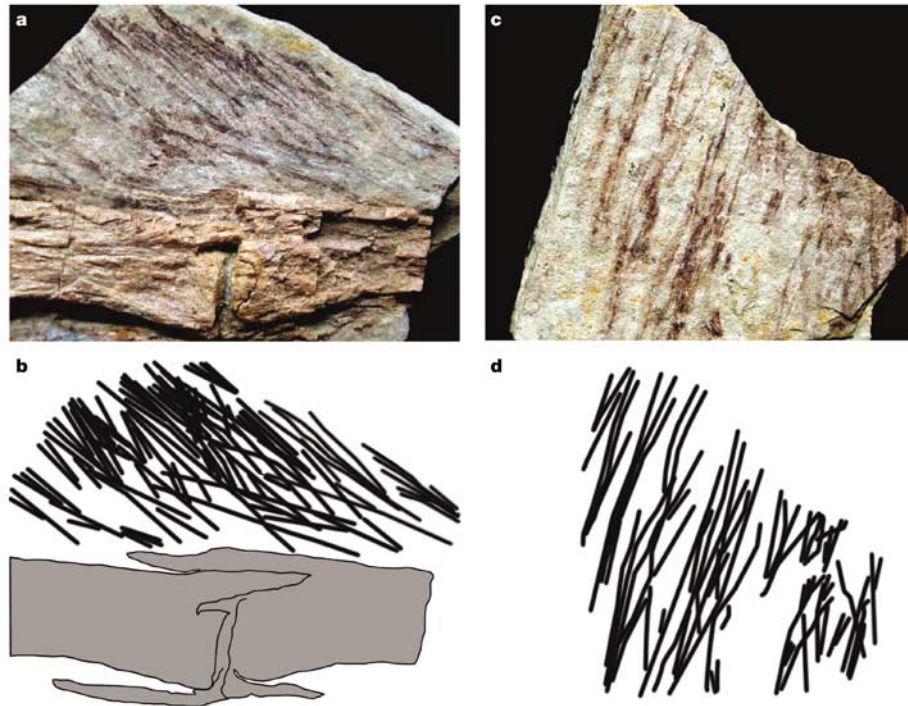


**Figure 3** Integumentary structures of IVPP V11579. **a, b**, Filamentous integumentary structures along the dorsal edge of the distal caudal vertebrae, photograph (**a**) and

linedrawing (**b**). **c, d**, Close-up of the integumentary structures showing the simple branching pattern, photograph (**c**) and linedrawing (**d**). Not to scale.

Several features are significant for understanding coelurosaurian evolution. In comparison with the gigantic, derived Late Cretaceous tyrannosauroids, Liaoning tyrannosauroids have a less pneumatic skeleton. Postcranial pneumatization is, as in tyrannosauroids, also less developed in small, basal members of many non-avian coelurosaurian groups<sup>15,24</sup> and more developed in large, derived members of these groups. The distribution of postcranial pneumatization is thus very complex among coelurosaurians<sup>15,24</sup>, rather than displaying a continuous evolutionary trend along the line to birds. Liaoning tyrannosauroids lack an arctometatarsalian pes, a feature often suggested to be associated with a strong cursorial capability<sup>19</sup>. The arctometatarsalian pes has been proposed to diagnose a more inclusive group, Arctometatarsalia<sup>25</sup>. However, recent discoveries show that this interesting pedal feature, as in tyrannosauroids, is absent from small, basal members of most 'arctometatarsalian' subgroups<sup>15,26</sup>, and is developed in the derived, larger members of the respective groups. In other taxa such as alvarezsaurids and troodontids, the arctometatarsalian pes is present even in small-bodied forms. This strongly supports the hypothesis that the arctometatarsalian pes evolved independently within different coelurosaurian groups<sup>21,27</sup>.

The filamentous integumentary structures in Jehol theropods have been interpreted as protofeathers<sup>22</sup>. The presence of the similar structures in IVPP V11579 provides the first direct evidence showing that tyrannosauroids possessed protofeathers. Furthermore, the filamentous protofeathers are branched as in other coelurosaurians<sup>22</sup>. This is a distinctive morphological feature of modern feathers, suggesting that this important modification occurred early in coelurosaurian evolution. Large, derived tyrannosauroids were reported to have scaled skin<sup>28</sup>, but the presence of two kinds of body covering is not unexpected. However, current understanding of the integumentary morphology in non-avian theropods is hindered by poor information on distribution. Given the diverse morphologies of integumentary structures in living birds, it is possible that non-avian theropods had different integumentary morphologies on different regions of the body, and derived, large

tyrannosauroids might bear both scale-like and filamentous integumentary appendages. Alternatively, the lack of filamentous integumentary structures in derived tyrannosauroids is correlated with the large size, a physiological strategy also adopted by some mammals such as elephants, which lose most of their body hairs as they mature<sup>29</sup>. This therefore supports the hypothesis that the original function of protofeathers is correlated with thermoregulation<sup>30</sup>. □

Received 18 May; accepted 13 July 2004; doi:10.1038/nature02855.

- Holtz, T. R. Jr in *Mesozoic Vertebrate Life* (eds Carpenter, K. & Tanke, D.) 64–83 (Indiana University Press, Bloomington, 2001).
- Currie, P. J., Hurum, J. H. & Sabath, K. Skull structure and evolution in tyrannosaurid dinosaurs. *Acta Palaeontol. Pol.* **48**, 227–234 (2003).
- Currie, P. J. Cranial anatomy of tyrannosaurid dinosaurs from the Late Cretaceous of Alberta, Canada. *Acta Palaeontol. Pol.* **48**, 191–226 (2003).
- Hurum, J. H. & Sabath, K. Giant theropod dinosaurs from Asia and North America: skulls of *Tarbosaurus bataar* and *Tyrannosaurus rex* compared. *Acta Palaeontol. Pol.* **48**, 161–190 (2003).
- Brochu, C. A. Osteology of *Tyrannosaurus rex*: insights from a nearly complete skeleton and high-resolution computed tomographic analysis of the skull. *J. Vertebr. Paleontol. Mem.* **7**, 1–138 (2003).
- Buffetaut, E., Suteethorn, V. & Tong, H. The earliest known tyrannosaur from the Lower Cretaceous of Thailand. *Nature* **381**, 689–691 (1996).
- Manabe, M. The early evolution of Tyrannosauridae in Asia. *J. Paleontol.* **73**, 1176–1178 (1999).
- Hutt, S., Naish, D., Martill, D. M., Barker, M. J. & Newbery, P. A preliminary account of a new tyrannosaurid theropod from the Wessex Formation (Early Cretaceous) of southern England. *Cretaceous Res.* **22**, 227–242 (2001).
- Rauhut, O. W. M. A tyrannosaurid dinosaur from the Upper Jurassic of Portugal. *Palaentology* **46**, 903–910 (2003).
- Swisher, C. et al. Further support for a Cretaceous age for the feathered-dinosaur beds of Liaoning, China: new <sup>40</sup>Ar/<sup>39</sup>Ar dating of the Yixian and Tuchengzi formations. *Chin. Sci. Bull.* **46**, 2009–2013 (2001).
- Erickson, G. M. et al. Gigantism and comparative life history of *Tyrannosaurus rex*. *Nature* **430**, 772–775 (2004).
- Molnar, R. E. The cranial morphology of *Tyrannosaurus rex*. *Palaentographica A* **217**, 137–176 (1991).
- Currie, P. J. & Dong, Z. New information on *Shanshanosaurus huoyanshanensis*, a juvenile tyrannosaurid (Theropoda, Dinosauria) from the Late Cretaceous of China. *Can. J. Earth Sci.* **38**, 1729–1737 (2001).
- Sampson, S. D. et al. Predatory dinosaur remains from Madagascar: implications for the Cretaceous biogeography of Gondwana. *Science* **280**, 1048–1051 (1998).
- Xu, X. *Deinonychosaurian Fossils from the Jehol Group of Western Liaoning and the Coelurosaurian Evolution* Thesis, Chinese Academy of Sciences, Beijing (2002).
- Currie, P. J. New information on the anatomy and relationships of *Dromaeosaurus albertensis* (Dinosauria: Theropoda). *J. Vertebr. Paleontol.* **15**, 576–591 (1995).
- Madsen, J. H. *Allosaurus fragilis*: a revised osteology. *Utah Geol. Min. Surv. Bull.* **109**, 1–163 (1976).

18. Gauthier, J. in *The Origin of Birds and the Evolution of Flight* (ed. Padian, K.) 1–55 (California Academy of Sciences, San Francisco, 1986).
19. Holtz, T. R. The arctometatarsalian pes, an unusual structure of the metatarsus of Cretaceous Theropoda (Dinosauria: Saurischia). *J. Vertebr. Paleontol.* **14**, 480–519 (1995).
20. Currie, P. J. Allometric growth in tyrannosaurids (Dinosauria: Theropoda) from the Upper Cretaceous of North America and Asia. *Can. J. Earth Sci.* **40**, 651–665 (2003).
21. Holtz, T. R. Jr A new phylogeny of the carnivorous dinosaurs. *Gaia* **15**, 5–61 (2000).
22. Xu, X., Zhou, H. H. & Prum, R. O. Branched integumental structures in *Sinornithosaurus* and the origin of feathers. *Nature* **410**, 200–204 (2001).
23. Carr, T. D. Craniofacial ontogeny in Tyrannosauridae (Dinosauria, Theropoda). *J. Vertebr. Paleontol.* **19**, 497–520 (1999).
24. Hwang, S. H., Norell, M. A., Ji, Q. & Gao, K. New specimens of *Microraptor zhaoianus* (Theropoda: Dromaeosauridae) from northeastern China. *Am. Mus. Novit.* **3381**, 1–44 (2002).
25. Holtz, T. R. The phylogenetic position of the Tyrannosauridae: implications for the theropod systematics. *J. Paleontol.* **68**, 1100–1117 (1994).
26. Xu, X., Norell, M. A., Wang, X. L., Makovicky, P. J. & Wu, X. C. A basal troodontid from the Early Cretaceous of China. *Nature* **415**, 780–784 (2002).
27. Sereno, P. C. The evolution of dinosaurs. *Science* **284**, 2137–2147 (1999).
28. Martin, L. D. & Czerkas, S. A. The fossil record of feather evolution in the Mesozoic. *Am. Zool.* **40**, 687–694 (2000).
29. Spingale, C. *Elephants* (T. & A.D. Poyser, London, 1994).
30. Chen, P. J., Dong, Z. M. & Zhen, S. N. An exceptionally well-preserved theropod dinosaur from the Yixian Formation of China. *Nature* **391**, 147–152 (1998).

Supplementary Information accompanies the paper on [www.nature.com/nature](http://www.nature.com/nature).

**Acknowledgements** We thank T. Holtz, O. Rauhut and X.-C. Wu for critical comments on the manuscript; Z. H. Zhou, Z. L. Tang, Y. Q. Wang, Y. Li, H. J. Wang, Y. L. Huo, H. Q. Shou, X.Z. Liu, Q. Cao, W. Chen, J. C. Lu and C. Li for their contribution in the field; H. J. Wang, J. M. Yang, G. H. Cui and X. Q. Ding for preparing the specimens; and R. S. Li, J. L. Huang and M. W. Yang for illustrations. The study was supported by the Special Funds for Major State Basic Research Projects of China, the National Natural Science Foundation of China, the National Geographic Society, the Chinese Academy of Sciences, the National Science Foundation of the USA and the American Museum of Natural History.

**Competing interests statement** The authors declare that they have no competing financial interests.

**Correspondence** and requests for materials should be addressed to X.X. ([xu@amnh.org](mailto:xu@amnh.org) or [xingxu@vip.sina.com](mailto:xingxu@vip.sina.com)) or M.A.N. ([norell@amnh.org](mailto:norell@amnh.org)).

## Pleistocene to Holocene extinction dynamics in giant deer and woolly mammoth

A. J. Stuart<sup>1</sup>, P. A. Kosintsev<sup>2</sup>, T. F. G. Higham<sup>3</sup> & A. M. Lister<sup>1</sup>

<sup>1</sup>Department of Biology, University College London, London WC1E 6BT, UK

<sup>2</sup>Institute of Plant and Animal Ecology, 620144 Ekaterinburg, Russia

<sup>3</sup>Oxford Radiocarbon Accelerator Unit, University of Oxford, Oxford OX1 3JQ, UK

The extinction of the many well-known large mammals (mega-fauna) of the Late Pleistocene epoch has usually been attributed to ‘overkill’ by human hunters, climatic/vegetational changes or to a combination of both<sup>1,2</sup>. An accurate knowledge of the geography and chronology of these extinctions is crucial for testing these hypotheses. Previous assumptions that the mega-fauna of northern Eurasia had disappeared by the Pleistocene/Holocene transition<sup>2</sup> were first challenged a decade ago by the discovery that the latest woolly mammoths on Wrangel Island, northeastern Siberia, were contemporaneous with ancient Egyptian civilization<sup>3,4</sup>. Here we show that another spectacular mega-faunal species, the giant deer or ‘Irish elk’, survived to around 6,900 radiocarbon yr BP (about 7,700 yr ago) in western Siberia—more than three millennia later than its previously accepted terminal date<sup>2,5</sup>—and therefore, that the reasons for its ultimate demise are to be sought in Holocene not Pleistocene events. Before their extinction, both giant deer and woolly mammoth

underwent dramatic shifts in distribution, driven largely by climatic/vegetational changes. Their differing responses reflect major differences in ecology.

The giant deer, *Megaloceros giganteus* Blumenbach, with a maximum shoulder height of 2.1 m and an antler span of up to 3.6 m, is one of the most striking and evocative extinct animals of the Palaearctic. First appearing about 0.4 Myr ago<sup>6</sup>, the overall distribution of *M. giganteus* during the Last Cold Stage extended across the middle latitudes of Eurasia from Ireland to east of Lake Baikal<sup>7</sup>. Its anatomy and distribution suggest it was a mixed feeder, requiring both to browse and to graze in a productive environment—especially necessary to sustain the annual antler growth in males<sup>6,8</sup>. On the other hand, it is likely that the huge antlers would have excluded males from even moderately dense woodland, at least for part of the year.

The giant deer was a key element in the relatively restricted set of Late Pleistocene extinctions in northern Eurasia, but unlike the mammoth it was not a species of the treeless ‘steppe–tundra’. Theories of its extinction formerly invoked the ‘maladaptation’<sup>9</sup>, or more recently the seasonal nutrient requirements<sup>8</sup>, of the huge antlers, and have focused on the well-studied Irish population of the Allerød phase around 12–10.6 kyr (12,000 to 10,600 uncalibrated radiocarbon yr BP; all dates hereafter are radiocarbon yr BP, unless stated otherwise. See Supplementary Information for calibrated calendar equivalents). Ireland has yielded most of the best-preserved specimens, including near-complete skeletons, from calcareous lake sediments ideal for the preservation of bone<sup>10,11</sup>. The absence of specimens from deposits of the succeeding Younger Dryas phase (about 10.6–10 kyr) has led to an extrapolated assumption of global extinction at the onset of this severe cold episode<sup>5,9,10</sup>.

Fortunately, most Late Quaternary extinctions occurred well within the range of radiocarbon (<sup>14</sup>C) dating, and we use direct dating of megafaunal remains, thereby minimizing any uncertainties of stratigraphical context. So far we have obtained 43 new radiocarbon accelerator mass spectrometry (AMS) dates from the Oxford Radiocarbon Accelerator Unit (ORAU) directly from *M. giganteus* material from western Europe, the Urals and Siberia, to which have been added 49 previously published direct dates (ORAU and other laboratories) (see Supplementary Information). This direct-dating approach has allowed us to track the fate of the species through climatic episodes leading up to extinction across its geographic range and in relation to changing palaeoenvironments.

During the Last Cold Stage, until around 20 kyr, the giant deer was widespread across western Europe (Fig. 1a), although the records are sporadic, and to the north of the Mediterranean region its occurrence may have been restricted to warmer (interstadial) phases with suitable vegetational growth. Indirectly dated records suggest that the species was probably also present in southeastern Europe and central Asia<sup>12</sup> during this time, and there are two dates around 39 kyr and 41 kyr (close to or beyond the reliable limit of <sup>14</sup>C dating) from Kamenka Buryatia, Transbaikalia (Supplementary Information). However, there are no known occurrences before 20 kyr from the Urals and the adjacent part of western Siberia.

Our data so far indicate a striking absence of dates for giant deer within the long interval around 20–12.5 kyr, implying that it had withdrawn entirely from western and central Europe. This period corresponds broadly to the Last Glacial Maximum (LGM), when the Scandinavian and Alpine ice sheets expanded, and elsewhere open treeless steppe–tundra vegetation predominated. Indirectly dated records<sup>12</sup> suggest that refugia for *Megaloceros* at this time (Fig. 1b) included parts of southeastern Europe and south central Asia, probably in areas where tree and shrub vegetation persisted. So far there are no records for giant deer, <sup>14</sup>C-dated or otherwise, from Mediterranean Europe for the LGM period, although in view of the known persistence of woodland<sup>13</sup> (Supplementary Information) this region presumably would have provided suitable refugia for this animal.